Agricultural and Forest Meteorology 248 (2018) 240–250

Contents lists available at ScienceDirect

Agricultural and Forest Meteorology

journal homepage: www.elsevier.com/locate/agrformet

Research paper

Assessing spring frost effects on beech forests in Central Apennines from remotely-sensed data

Marco Bascietto[a], Sofia Bajocco[b,*], Francesco Mazzenga[c], Giorgio Matteucci[d]

[a] Council for Agricultural Research and Economics (CREA), Research Centre for Engineering and Agro-Food Processing, Rome, Italy
[b] Council for Agricultural Research and Economics (CREA), Research Centre for Agriculture and Environment, Rome, Italy
[c] National Research Council, Institute of Agro-Environmental and Forest Biology (CNR-IBAF), Monterotondo, Italy
[d] National Research Council, Institute for Agricultural and Forestry Systems in the Mediterranean (CNR-ISAFOM), Ercolano, Italy

ARTICLE INFO

Keywords:
Spring frost
Common beech forest
MODIS EVI
Net ecosystem exchange

ABSTRACT

In common beech forests the most damaging frosts are those that occur at the end of spring. At that time the fresh new leaves are at a vulnerable stage and risk to be readily killed by the freezing temperatures. The ability to identify late spring frost spatial dynamics is a key issue for understanding forest patterns and processes linked to such extreme event. The aim of this study is to detect, map and quantify the vegetation anomalies that occurred in the mono-specific beech forest of the Lazio, Abruzzo and Molise National Park (Italy) after an exceptional spring frost recorded on the 25th of April 2016. Results showed that, beech forests at lower elevations that had an early greening process were subject to spring frost damage (SFD pixels) and their productivity performance strongly decreased with respect to the previous 15 years; to the contrary the beech forests located at higher elevations did not suffer the spring frost effects (NSFD pixels) thanks to their delayed leaf unfolding phase. The duration of the effects of freezing stress for the SFD pixels was about two months, until the end of June, confirmed by Net Ecosystem Exchange measurements. This greening hiatus led to an average 14% loss of productivity compared to the previous 15 years. Elevation had a significant role on the probability of occurrence of SFD pixels. Productivity loss in SFD pixels was more severe at elevations in the range 1500–1700 m, on steeply terrains and North aspects. This study represents a step forward the systematic use of automated techniques to study areas subject to stress or anomalies from multitemporal satellite imagery and to identify break points and recovery of the greening process.

1. Introduction

With climate change, in Central Europe, the start of the growing season has advanced over the last decades (Badeck et al., 2004); over three decades, leaf unfolding has started 6 days earlier (Menzel and Fabian, 1999; Muffler et al., 2016). The frequency of cold spells in spring is likely to decrease (Menzel et al., 2015); however, leaf unfolding is also projected to occur much earlier (Rosenzweig et al., 2008) with potential negative impacts to productivity (Kim et al., 2014).

Extreme cold events after an earlier growing season onset are increasing the risk of frost damage in the temperate zone (Inouye, 2000; Hufkens et al., 2012; Augspurger, 2013; Muffler et al., 2016). The timing of spring phenological development plays a crucial role, not only at the species level, but also at the individual and population level (Menzel et al., 2015).

Common beech (*Fagus sylvatica* L.), the naturally dominant forest tree species of Central Europe over a wide range of environmental conditions (Leuschner et al., 2006), can tolerate very cold conditions over winter, but is sensitive to late frost events (Ningre and Colin, 2007; Kreyling et al., 2012a) more than other tree species due to the earlier onset of leaf unfolding (Dittmar et al., 2006). The ability to identify spring frost spatial dynamics and quantify their damages in term of productivity loss is hence crucial for understanding climate-driven altitudinal shifts.

While probabilistic field measurements of forest productivity may optimise sampling times (Bascietto et al., 2012), remotely-sensed vegetation indices like NDVI (Normalized Difference Vegetation Index) and EVI (Enhanced Vegetation Index) are regarded as reliable indicators for estimating productivity and monitoring vegetation conditions globally (see, e.g., Myneni and Williams, 1994; Cuomo et al., 2001; Lanfredi et al., 2003; Bajocco et al., 2012). NDVI is the most common vegetation index used to monitor vegetation; however there are still some limitations in the NDVI product related to the index saturation in densely-vegetated areas, and to the effect of canopy

* Corresponding author.
E-mail address: sofia.bajocco@crea.gov.it (S. Bajocco).

http://dx.doi.org/10.1016/j.agrformet.2017.10.007
Received 29 May 2017; Received in revised form 26 September 2017; Accepted 5 October 2017
Available online 07 October 2017
0168-1923/

background (Wang et al., 2003).EVI was hence proposed as a modified NDVI allowing more responsiveness to canopy structural variations, including leaf area index (LAI) in forests (Huete et al., 2002).EVI is useful for monitoring seasonal and inter-annual dynamics of vegetation (Huete et al., 2002), for predicting net primary production in ecosystem modeling applications (Potter et al., 2007; Maeda et al., 2014); for quantifying the extent of the shifts in vegetation phenology between rural and urban areas (Dallimer et al., 2016); for examining the relationships between seasonal rainfall fluctuations and phenological parameters (Suepa et al., 2016).

In remote sensing, the analysis of anomalies associated to environmental stress has been performed by means of many different approaches. Anomaly regions in satellite images can reflect unexpected variations of vegetation cover caused by land use changes, fire, landslide, drought, disease, etc.

Zhou et al. (2016), in order to identify land cover dynamic processes, proposed a method for detecting anomaly regions in each NDVI time series image based on seasonal autocorrelation analysis. Yool (2001) enhanced fire scar anomalies by applying the Z-transform on NDVI time-series data; the multi-temporal Z (MTZ) score image thus depicts any deviation of a given pixel, for a specific step in the series, relative to the mean for that pixel across the time series. Fraser and Latifovic (2005) developed a logistic regression model based on satellite change metrics to map insect-induced defoliation and mortality over a coniferous forest region in Quebec (Canada) by means of NDVI and other VIs. Olsson et al. (2016), in order to monitor insect disturbances in Finnish forests, used a damage detection method based on z-scores of seasonal maximums of the 2-band EVI data. Mildrexler et al. (2007) developed a pixel-based algorithm based on the consistent radiometric relationship between Land Surface Temperature and EVI to automatically and systematically detect disturbance at global scale. Menzel et al. (2015) analyzed the greenness time series by a Bayesian multiple change point modeling. Van Hoek et al. (2016) applied a Fourier method to model NDVI time series affected by gaps and outliers (iHANTS). Finally, Lasaponara (2006) focused on the extraction of vegetation inter-annual anomalies from a NDVI temporal series (1999–2002) by applying principal component analysis as a data transformation to enhance regions of localized change in multi-temporal data sets.

In this study, to exploit the EVI capabilities of measuring phenological anomalies in densely-vegetated regions, we developed an automated approach to detect areas of late frost damage from EVI satellite imagery based on machine learning (ML) techniques. ML is a method of data analysis that automates analytical model building, using algorithms that iteratively learn from data.

The investigation focuses on a mono-specific common beech forest of the Lazio, Abruzzo and Molise National Park, Central Apennines (Italy), where an unprecedented severe spring frost occurred on 25th April 2016. The main objectives of this study therefore are: (i) to identify all the areas within the study region where the spring frost anomaly occurred based on EVI annual profiles; (ii) to estimate how topographic factors influenced the occurrence of the damages; (iii) to quantify the productivity loss of 2016 compared to the previous 15 years.

2. Study area

Lazio, Abruzzo and Molise National Park (LAMNP) is an Italian national park founded in 1922 (Fig. 1). The majority of the park is located in the Abruzzo region though it is not constrained by regional boundaries and also includes territory in Lazio and Molise. The park currently covers 496.80 km^2. The morphology is predominantly mountainous, with the highest peak at 2249 m (Petroso Mtn.) The flora of the park is extremely rich with more than 2000 species. European common beech (*Fagus sylvatica* L.) forest covers 60% of the area and dominates the park between 1400 and 1900 m.

A Long-Term Ecosystem Research site (Collelongo-Selvapiana LTER_EU_IT_031, lat. 41.84936 N, long. 13.58814 E, 1560 m asl) is located in the protection belt of LAMNP. The site performs flux measurements with eddy covariance since 1995 in a mono-specific common beech forest (https://data.lter-europe.net/deims/site/lter_eu_it_031) and, on the 25th April 2016, it experienced an anomalous spring frost that damaged nearly 100% of developing shoots and expanding leaves of canopy trees (Fig. 2). The spring frost followed an unprecedented warm period, as detected by 8-day MODIS Terra Nighttime Land Surface Temperature (LST)/Emissivity (MOD11A2) product. The comparison of the LST of 2016 versus the previous 15 years (2001–2015) highlighted that an anomalous early spring warm period occurred since DOY 81 (March, 21st) followed by a sudden below zero drop in temperature on DOY 113 (April, 22nd) (Fig. 3).

3. Data

3.1. MODIS vegetation index

The 16-day MODIS Terra 250 m EVI maximum value composite product (MOD13Q1) was downloaded from the MODIS SOAP Web Service, covering the whole LAMNP and its protection belt for the 15 year-long period 2001–2016. Winter data revealed several low quality, noisy or out of valid range value regions, therefore the late-autumn and winter data of each year were excluded from the analysis. We focused only on the EVI temporal profiles starting from day of year (DOY) 81 (21st of March) to 305 (1st of November), which encompasses the growing season of the European beech forest.

4. Methods

4.1. Training of the SFD-NSFD classifier

A support vector machine (SVM) was used to detect pixels of spring frost damage in EVI data. SVM is a supervised learning model that works as a discriminative classifier formally defined by a separating hyperplane. The training data consist of a set of training examples. Given labeled training data, the algorithm outputs an optimal hyperplane which categorizes new examples into one class or the other (James, 2003; Campbell and Ying, 2010).

A region of 33 × 33 pixels centered at the LTER_EU_IT_031 site (4 km on the right and 4 km on the left from the site pixel) was identified as “training site” for the SVM classifier; this size was chosen in order to be consistent with the LTER_EU_IT_031 site information about the 2016 spring frost occurrence and to avoid the inclusion of adjacent non-forested areas.

To extract only the pure (phenologically homogeneous) beech forest pixels within the training site, a k-means clustering was performed on the 2001–2015 (no spring frost events detected) EVI profiles data.

The k-means clustering is an unsupervised classification technique; it calculates initial class means evenly distributed in the data space, then iteratively clusters the pixels into the nearest class using a minimum distance technique. This process continues until the number of pixels in each class changes by less than the selected pixel change threshold or the maximum number of iterations is reached (MacQueen, 1967; Bajocco et al., 2012). The k-means clustering procedure was used to cluster the vegetation of the training site into k homogeneous groups in terms of annual EVI profile; k was selected according to an iterative to convergence reallocation method starting with 2–5 clusters that resulted in an optimal number of 3 clusters. Given that the LTER_EU_IT_031 site is located in a mono-specific beech forest, the cluster that included LTER_EU_IT_031 site pixel was labeled as “beech forest” and the other two clusters as “non-beech forest” and excluded from the following analysis.

For the “beech forest” cluster of the training site, the EVI profile of the pixels for the year 2016 was taken as representative of the pixels

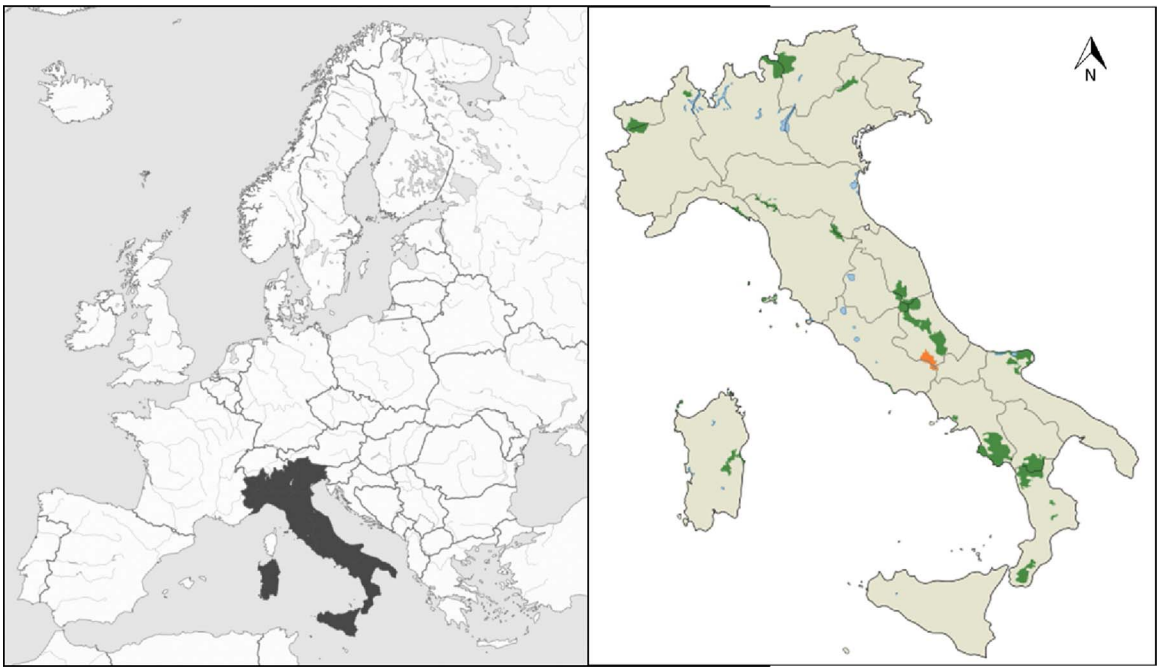

Fig. 1. Location of the study area: in green all the National Parks of Italy, in orange the Lazio, Abruzzo and Molise National Park (LAMNP). (For interpretation of the references to colour in this figure legend, the reader is referred to the web version of this article.)

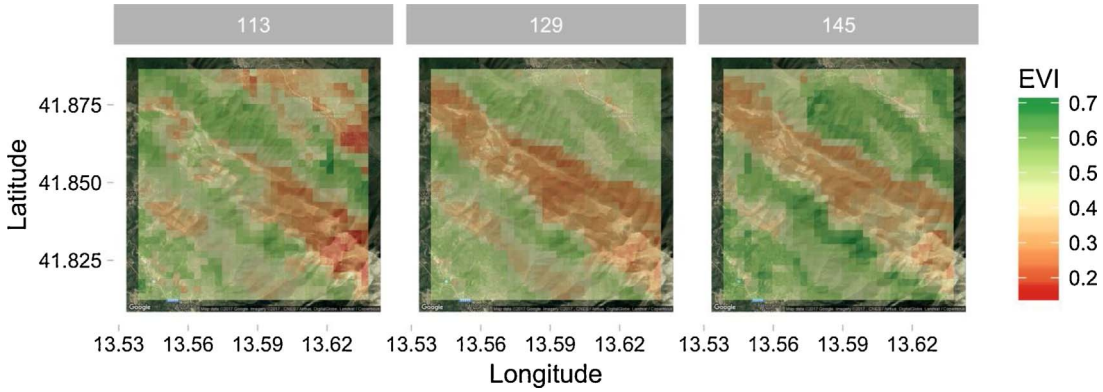

Fig. 2. Satellite view of the training site (LTER_EU_IT_031 site is in the centre of map) and its EVI values, just before (DOY 113, 22nd April) and after (DOY 129 and DOY 145, 8th and 24th May respectively) the year 2016 spring frost event.

subject to spring frost damage (SFD − anomaly), while the EVI profiles of the pixels for the years 2001–2015 were taken as representative of the pixels where no spring damage occurred (NSFD − normality). Both datasets (anomaly and normality) were randomly divided in two portion: 70% trained the classification model, the remaining 30% tested the classifier accuracy.

4.2. Application of the SFD − NSFD classifier

We identified a 60 km x 50 km bounding box, named “application area”, covering the LAMNP boundaries and including the LTER_EU_IT_031 site, whose central point coordinates are Lat. 41.8108 N, Long. 13.782 E. The size of the application area was chosen to ensure that the growth process and timing of the beech forests within the training site and within the application area were comparable.

In order to apply (and test) the trained classifier on the whole LAMNP region covered by beech forests, within the application area we delimited the European beech distribution range according to three data sources: (i) the Forest Type Cover (FTY) of the Copernicus Land Monitoring Service (http://land.copernicus.eu/pan-european/high-resolution-layers/forests); (ii) the Digital Elevation Model (DEM) of the GMES RDA project, (http://www.eea.europa.eu/data-and-maps/data/eu-dem#tab-original-data); (iii) the EUFORGEN trees distribution range (http://www.euforgen.org/distribution-maps). Only those pixels belonging to FTY Broadleaf forest class, on an elevation between 1400 m and 1900 m, and included in the distribution range of *Fagus sylvatica* were considered as beech forest and further analyzed.

Finally, the trained classifier was applied to the 2016 EVI profiles of all the beech forest pixels of the application area. The SVM classified each pixel as being affected by the anomaly or not (SFD or NSFD).

In order to visually compare the seasonal profiles of affected and non-affected (nearby) pixels, we randomly selected three pairs of adjacent SFD/NSFD pixels and charted their year 2016 EVI time series.

4.3. Net ecosystem exchange estimation

Estimates of Net Ecosystem Exchange (NEE, μmol CO2 m-2 s-1), aggregated on a weekly basis, were used as a reference to compare the greening hiatus duration, estimated by MODIS EVI, after the spring frost occurrence. NEE is the flux variable directly measured using the eddy covariance technique in LTER_EU_IT_031 site (Matteucci et al., 2007; Mazzenga, 2017) on the basis of the turbulent flux (derived from

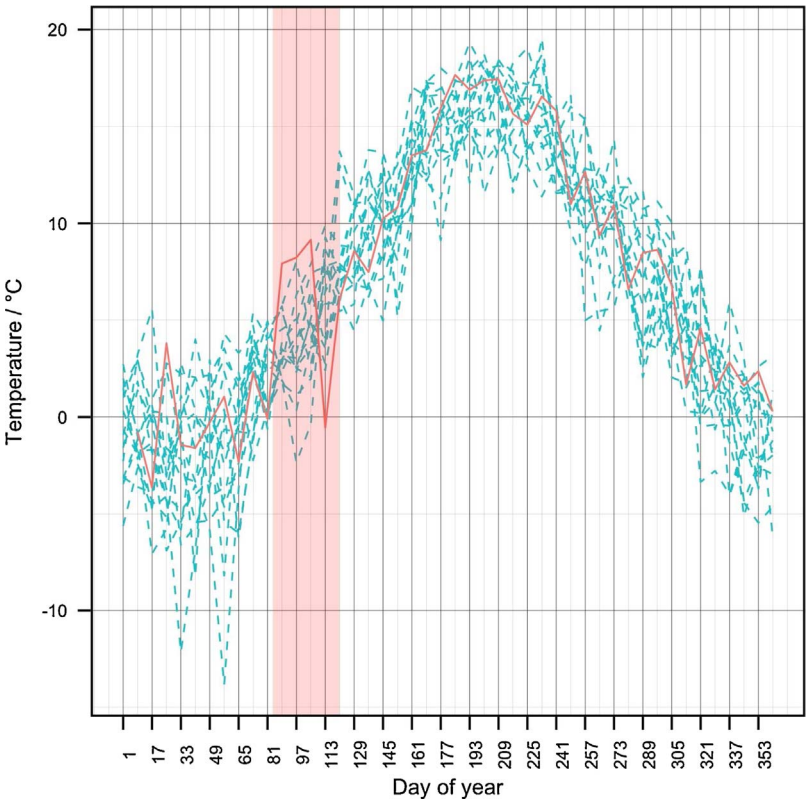

Fig. 3. MODIS Nighttime Land Surface Temperature (LST) 8-days composite data from 2001 to 2016. The red line highlights year 2016 LST, while cyan lines all the other years. The vertical red strip highlights the anomalous 2016 temperature trend before and during the frost event (DOY = 116, i.e. 25th of April). (For interpretation of the references to colour in this figure legend, the reader is referred to the web version of this article.)

the 20 Hz measurements of CO2 concentration and wind parameters) plus the storage component (Aubinet et al., 2012). Corrected vertical fluxes of CO2 were estimated using the software package EddyPro (LI-COR, v. 6.2.0) by removal of outliers and application of standard corrections, according to the standardized approaches of FluxNet (Aubinet et al., 2000).

4.4. Correlation between SFD pixels and topography

In order to test how the location of the anomalous (SFD) pixels within the beech range is influenced by the topography of the application area, a logistic binomial Generalized Linear Model (GLM) estimated the probability of a pixel be classified as being affected by SFD or not with elevation, aspect and slope as explanatory variables. For the aspect, due to the circularity of the variable, we used the North as reference. A chi-squared test was used to compute the deviance table for the GLM fit. The topographic variables were derived using the DEM of the GMES RDA project.

4.5. Correlation between SFD pixels and topography

In order to test how the location of the anomalous (SFD) pixels within the beech range is influenced by the topography of the application area, a logistic binomial Generalized Linear Model (GLM) estimated the probability of a pixel classified as being affected by SFD or not with elevation, aspect and slope as explanatory variables. For the aspect, due to the circularity of the variable, we used the North as reference. A chi-squared test was used to compute the deviance table for the GLM fit. The topographic variables were derived using the DEM of the GMES RDA project.

4.6. Comparison between 2016 and the previous 15 years

First, to test if the EVI temporal profile in 2016 is linearly correlated or not with the EVI profile of the previous 15 years (2001–2015), we performed a correlation analysis separately for the SFD and NSFD pixels. In order to give a statistical significance to the correlation analysis, for each pair formed by 2016 and one of the previous 15 years (2001–2015), we performed a *t*-test between the correlation coefficients of the SFD and the NSFD pixels.

Productivity at pixel level for each year was estimated by integrating MODIS MOD13Q1 EVI profiles over the DOY 81–305 time period (TOTEVI). MODIS MOD17A2H product directly offers GPP estimates, but its spatial resolution (500 m/px, 4 x lower than MOD13Q1) did not allow to render a detailed spatial map of frost damages over the application area. For each pixel, the productivity change due to the spring frost event was estimated using a productivity ratio (PR) by dividing the 2016 TOTEVI to TOTEVIs of each of the previous 15 years. PR values below 1 indicate that year 2016 productivity has been lower; PR values close to 1 indicate a balanced productivity; PR values higher than 1 indicate a higher productivity for year 2016.

Finally, in order to test if the productivity of 2016 is significantly different from the productivity of the previous years, for each pixel within the beech forest range, we performed a *t*-test between the TOTEVI of 2016 and the pool of TOTEVIs for the years 2001–2015, both for SFD and NSFD pixels. Null hypothesis was the difference between the two datasets (i.e. 2016 and 2001–2015) is zero.

4.7. Influence of topography on frost-induced productivity loss

The influence of topography on the productivity ratio of SFD pixels was assessed by means of a generalized additive mixed model (GAMM) with year as random intercept factor and elevation, slope, and aspect as fixed factors. An additive model was chosen since the relationship between elevation and PR was not linear. A mixed model was chosen to predict the PR-topography general relationship through removing the between-year variation from the variance component. The random intercept adds random variation to the intercept at each year level and is assumed to follow a normal distribution with expectation 0, and unknown variance.

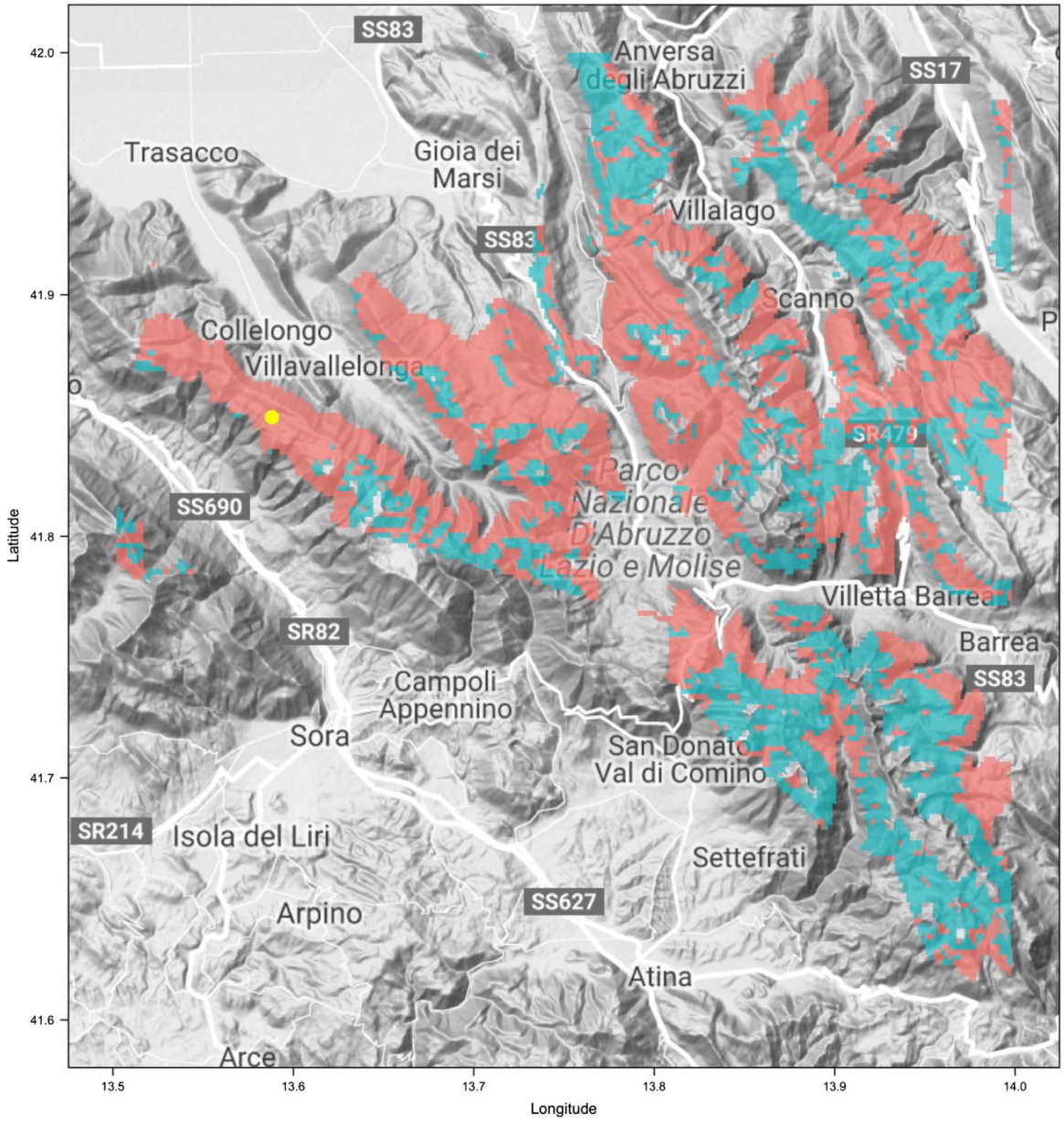

Fig. 4. Distribution of the SFD (red) e NSFD (cyan) pixels detected from the SVM within the European beech forest range across the application area (yellow dot pinpoints LTER_EU_IT_031 site pixel). (For interpretation of the references to colour in this figure legend, the reader is referred to the web version of this article.)

5. Results

Fig. 4 shows the distribution of the SFD e NSFD pixels within the common beech forest range across the application area. The pixels identified as being affected by SFD by the SVM are 5526 (345 km^2), while NSFD pixels are 3647 (227 km^2). The accuracy test on the confusion matrix provided an overall accuracy of 0.998, with the kappa coefficient equal to 0.981. The random selection of the three pairs of SFD and NSFD pixels showed that the EVI profiles of the SFD pixels generally follow an anomalous trend characterized by a spring increase followed by an abrupt decrease just after the frost event; to the contrary the EVI profiles of the NSFD pixels follow a regular seasonal trend, unaffected by the temperature anomaly (Fig. 5).

A logistic model (Table 1) show that elevation is negatively correlated with the probability of being affected by spring frost damage. Slope does not affect significantly SFD probability, while South and West facing terrains showed a slight negative influence on the probability of late frost damage to occur compared to North-facing terrains. Results from Chi-squared test show a major role of elevation (reduction of deviance 850) compared to aspect (reduction of deviance 125, Table 2).

The mean 2016 EVI trend for SFD and NSFD pixels within the beech distribution range of the application area followed different patterns (Fig. 6). EVI for SFD pixels was clearly higher and increasing at a higher pace than NSFD pixels, before spring frost occurrence. The damage in productivity of SFD pixels lasted for two months (from DOY 129 to DOY 193, e.g. from May, 8th to July, 11th). The earlier increase in EVI for SFD pixels points out an earlier onset of leaf unfolding than on NSFD pixels. The hiatus in productivity estimated by EVI is mirrored by the hiatus in Net Ecosystem Exchange measured in the footprint of the LTER_EU_IT_031 site (Fig. 7). Despite missing NEE measures during the first months of year, the site beech forest was a net source of Carbon into atmosphere all through June 2016 (DOY 177) signaling a complete interruption in vegetation activity, while it was expected to be a net Carbon sink. From July 2016 onwards the forest slowly recovered its vegetation activity by unfolding new leaves and, around mid August

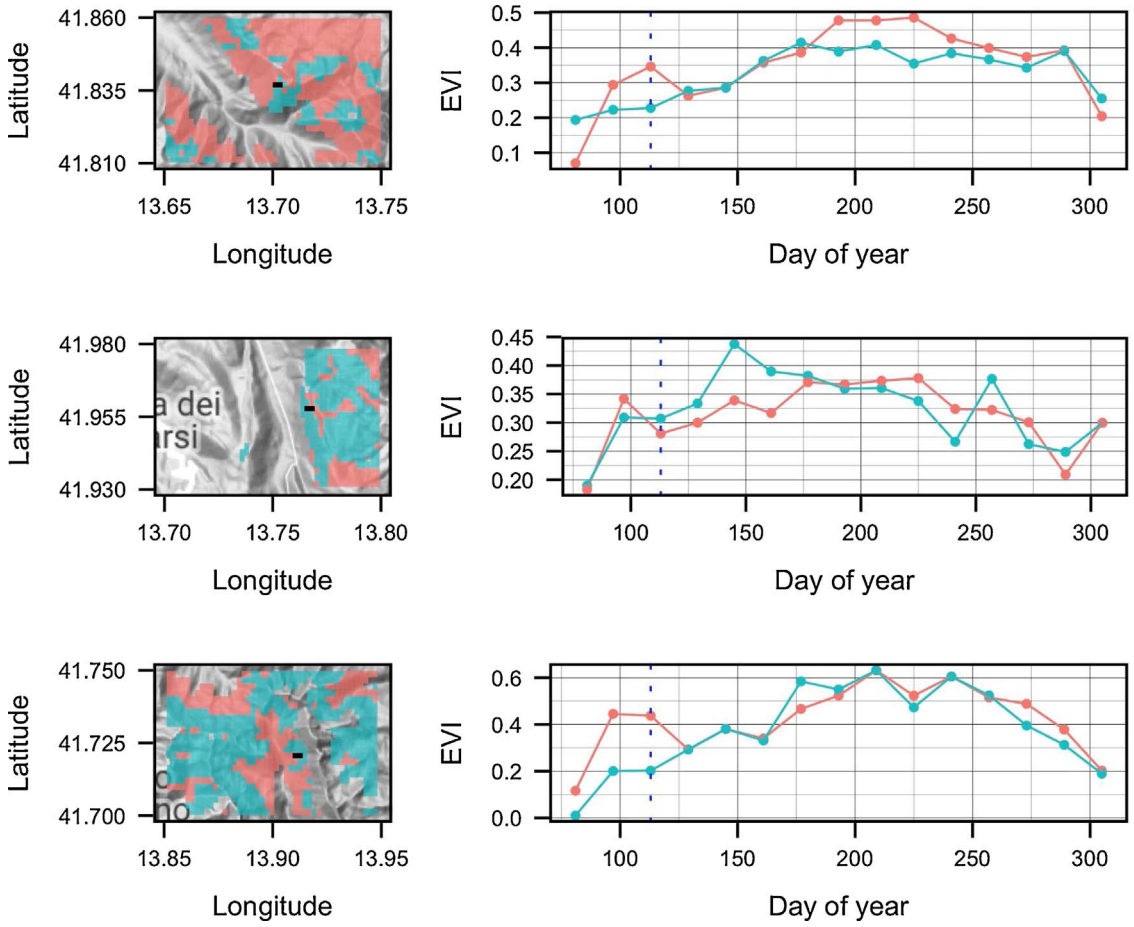

Fig. 5. EVI time series of three randomly selected adjacent pairs of SFD/NSFD pixels (pixels location on left side, time series on right side). SFD pixels are cyan-coloured, NSFD pixels are red-coloured. Spring frost DOY is highlighted as a dashed vertical line in time series plot.

Table 1
Values of estimate, standard error and z-statistic of the coefficient of the logistic binomial GLM to estimate the probability of a pixel to be affected by spring frost damage.

	estimate	std. error	z-statistic	p-value
(Intercept)	8.332	0.3020	27.59	< 0.001
Elevation	−0.0046	0.0002	−27.69	< 0.001
Aspect_East	0.0258	0.1036	0.2488	0.8035
Aspect_South	−0.5325	0.1045	−5.094	< 0.001
Aspect_West	−0.4530	0.1033	−4.387	< 0.001
Slope	−0.0003	0.0030	−0.0926	0.9262

Table 2
Analysis of deviance table for the logistic binomial GLM. DF = ° of freedom.

	DF	Residual deviance	p-value
Null		12296	
Elevation	1	11446	< 0.001
Aspect	3	11321	< 0.001
Slope	1	11321	0.9262

(DOY 225), it reached comparable NEE values to previous years.

The correlation coefficients analysis (Fig. 8) highlighted how the year 2016 EVI profile pattern of the SFD pixels was less correlated to previous years pattern (r = 0.6 on average) than the EVI pattern of NSFD pixels (r = 0.75 on average). The 2016 spring frost anomaly has affected the EVI annual profile of SFD pixels so that its pattern is significantly different from each and every year since 2001 ($p < 0.0001$).

SFD pixels in 2016 exhibit on average a loss of productivity (estimated as productivity ratio) with respect to the 15 previous years (PR < 1.0), unlike the NSFD pixels, that on average are characterized by a PR even higher than 1.0 (Fig. 9). Average year 2016 PR of NSFD pixels was 1.05, that is beech forest pixels not affected by the spring frost damage were on average 5% more productive than previous years. Average years 2016 PR of SFD pixels was 0.860: a 14% loss of productivity over previous years.

GAMM results showed that the productivity ratio of SFD pixels was unevenly affected by topographic factors (Table 3). GAMM parametric coefficient and smooth terms were significant ($p < 0.001$), explained variance was 25% (Adj. R^2 0.256). The fixed effects were not correlated; residuals did not show any pattern (Fig. 10, bottom panel).

Fig. 11 shows that year 2016 productivity was generally hindered by the spring frost in North-facing and in steep slope terrains. Spring frost damages to productivity were more severe at elevations in the range 1500–1700 m regardless of slope and aspect. The elevation threshold between SFD and NSFD forests on flat terrains was 1800 m in North aspects and 1750 m in South aspects. The threshold was about 50 m higher in steep terrains.

6. Discussion

Many studies so far have demonstrated that temporal series of remotely-sensed greenness indices are suitable for tracking the annual development of vegetation, in particular deciduous trees (Richardson et al., 2009; Zhang et al., 2006; Alberton et al., 2014), and also to capture and map extreme stress events, like droughts (e.g., Rojas et al., 2011; Assal et al., 2016). However, to the best of our knowledge, only a few studies so far have quantified the impact of a late spring frost event

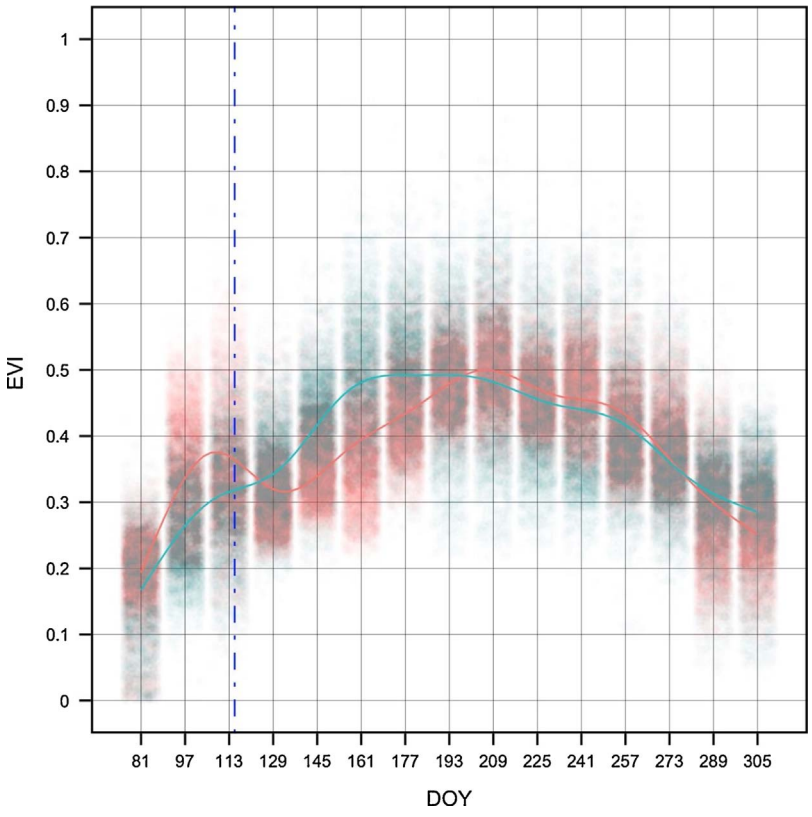

Fig. 6. 16-days composite EVI 2016 trend within the beech range of the application area. Cyan dots represent the NSFD pixels, while red dots represent the SFD pixels. The cyan line represents the mean EVI profile for the NSFD pixels, while the red line represents the mean EVI profile for the SFD pixels. Vertical segmented blue line represents the exact DOY of the spring frost event. (For interpretation of the references to colour in this figure legend, the reader is referred to the web version of this article.)

by remote sensing techniques (e.g., Lintvedt, 2011; Kim et al., 2014; Menzel et al., 2015).

The published literature agrees on the fact that the timing of a late spring frost event in relation to the actual phenological development stage would largely determine the damage caused (e.g. Rigby and Porporato, 2008). Late frost risk may hence be considered as a two stage problem: by responding to warmer temperatures in early spring, plants face a risk of temperature dropping below a damaging threshold after the onset of leaf unfolding (Rigby and Porporato, 2008). In common beech forests the most damaging frosts are those that occur at

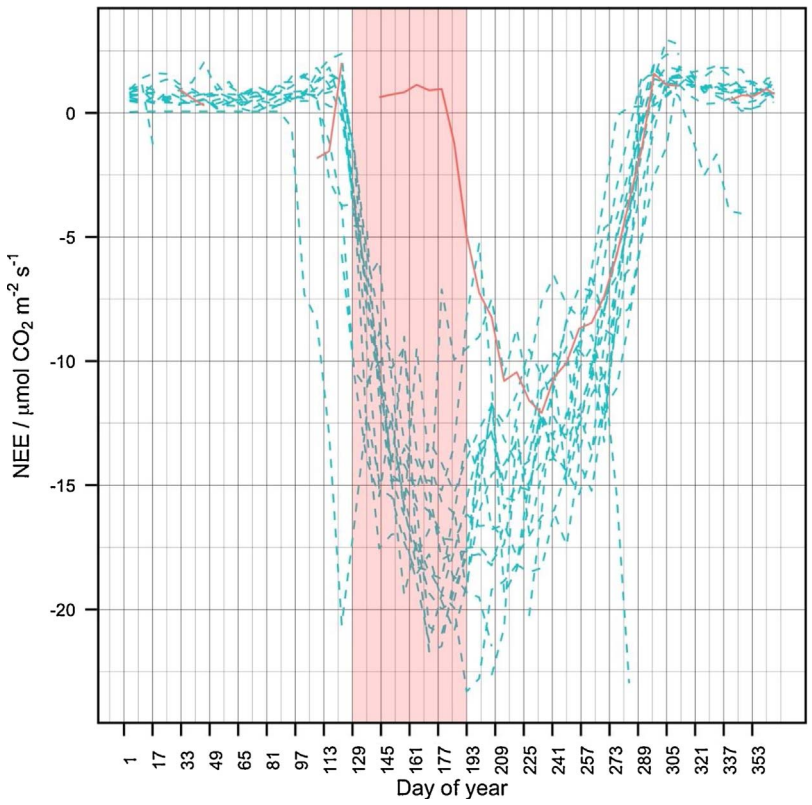

Fig. 7. Weekly aggregated half-hour, daytime, Net Ecosystem Exchange measured in LTER_EU_IT_031 site. Positive values mark a net Carbon emission, negative values mark a net Carbon assimilation by trees. The red line highlights year 2016 NEE, while cyan lines all the other years. The vertical red strip highlights the two months-long hiatus in productivity estimated by MODIS EVI that occurred just after the frost event (from DOY 129 to DOY 193). (For interpretation of the references to colour in this figure legend, the reader is referred to the web version of this article.)

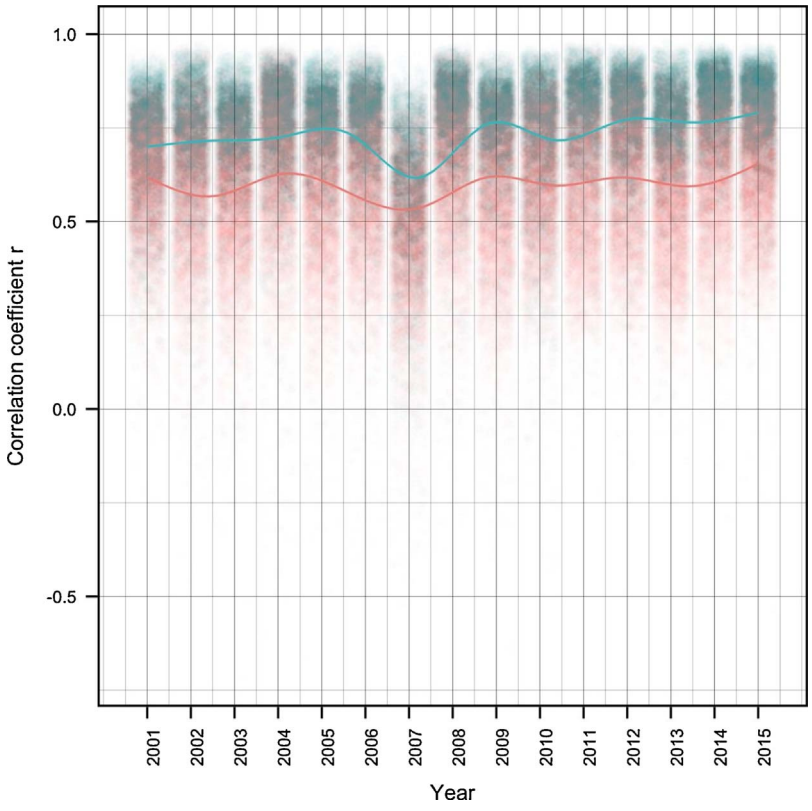

Fig. 8. Plot of the correlation coefficients between EVI 2016 trend and the previous years (2001–2015) patterns. In red, SFD pixels; in cyan, NSFD pixels. Lines are smoothed averages. (For interpretation of the references to colour in this figure legend, the reader is referred to the web version of this article.)

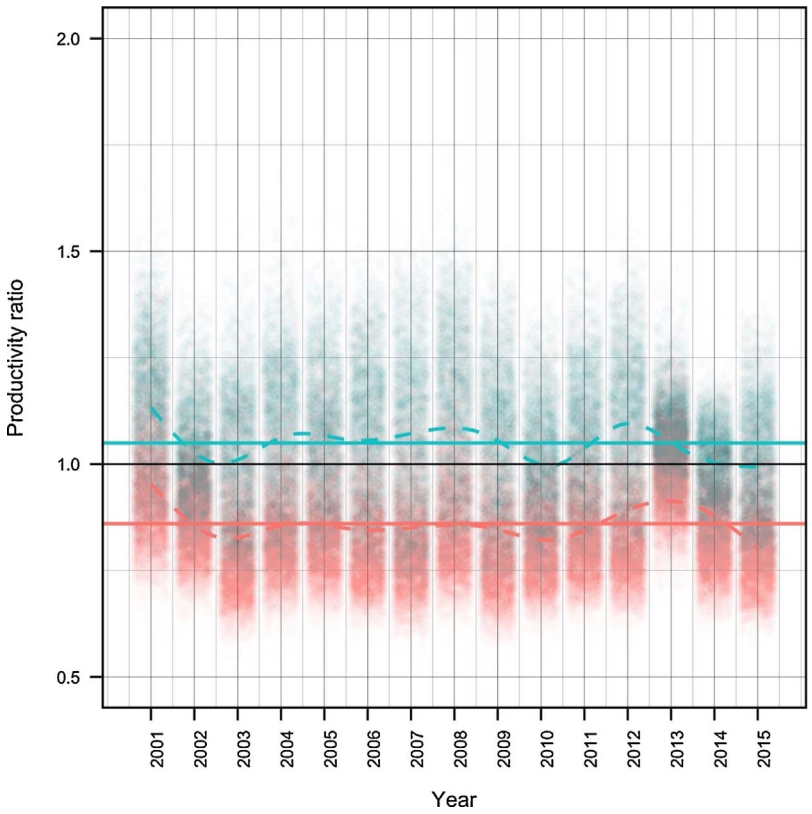

Fig. 9. Plot of the EVI productivity ratio between year 2016 and each of the previous years (2001–2015). In red, SFD pixels; in cyan, NSFD pixels. The horizontal lines represent the 15-years average productivity ratios (PRs). The dashed lines represent the yearly average PRs trend. (For interpretation of the references to colour in this figure legend, the reader is referred to the web version of this article.)

the end of spring. At that time the newly flushed shoots are at a vulnerable stage and are readily killed by the freezing temperatures. This can result in trees losing a whole year's growth, and repeated frost damage can kill trees or hold them in check for many years (Muffler et al., 2016).

In Central Europe, late frost events can occur until mid-May, with enormous effects on beech growth, (Dittmar et al., 2006; Menzel et al., 2015). In the worst cases, beech individuals lose their leaves entirely and are forced to rebuild them from stored resources. A few papers proved that the process of refoliation may take up to 36 days

Table 3
Random and fixed effects of the Mixed Model component of the GAMM with year as random effect, and smoothed elevation, aspect, and slope as fixed effects.

Random effects			
	Variance	Standard deviation	
(Intercept)	0.002	0.0451	
s(Elevation)	0.0618	0.2487	
s(Slope)	0.0933	0.3055	
s(Aspect)	0.007	0.0836	
Residual	0.0141	0.1189	
Fixed effects			
	Estimate	Std. Error	t value
(Intercept)	0.8601	0.0117	73.8
s(Elevation)	0.1038	0.0087	11.9
s(Slope)	−0.1239	0.0104	−11.9
s(Aspect)	−0.0148	0.0086	−1.72

(Scheifinger et al., 2003; Awaya et al., 2009), achieving again the status prior to frost after two months (Kreyling et al., 2012b). Such late frost events may even determine the northern and north-eastern range limit of common beech distribution (Bolte et al., 2007).

This study of a late spring frost event in a (mono-specific) beech stand in Central Italy, by remotely-sensed EVI data, confirms such considerations and contributes to understanding the phenological variations and subsequent enhanced susceptibility to a late frost event in a common beech forest that experienced an early greening trend.

According to the results obtained, in 2016, the late frost damage occurred in LAMNP due to two concurrent reasons: (i) the beech forest started its growing season earlier than previous years; (ii) a not uncommon frost happened on 25th of April, when the leaves were unfolding. As a result of the frost, the newly unfolded leaves collapsed and the beech forest stopped its greening development for almost two months, until the beginning of July as revealed by EVI profiles. This EVI time lag matches with the NEE lag registered in the present study and with the 7–9 weeks NDVI time lag estimated by Kreyling et al. (2012b) for spring frost damaged deciduous forests in southern Germany and with the time to "second greening" recorded by Menzel et al. (2015) in a beech forest in south-eastern Germany.

The 2016 spring frost heavily damaged the beech forests and their EVI profile patterns clearly recorded the phenomenon by showing an abrupt decrease in the vegetation index. The EVI profile pattern of year 2016 of SFD pixels was shown to be significantly different from each and every pattern of previous years (2001–2015) thus leading to confirm that the spring frost was the key to the anomaly in the EVI profile.

In this framework, the effect of elevation is clear and significant: the higher the elevation, the lower the probability of spring frost damage to the beech forest. Aspect has a significant (although weak) effect, in particular South and West facing terrains reduced the probability of spring frost damage to the forest. Higher elevation beech forests may have been preserved by the damages brought by the spring frost due to a delayed leaf unfolding phase granted to them by a cooler climate.

Year 2016 productivity in SFD beech forests was strongly affected at

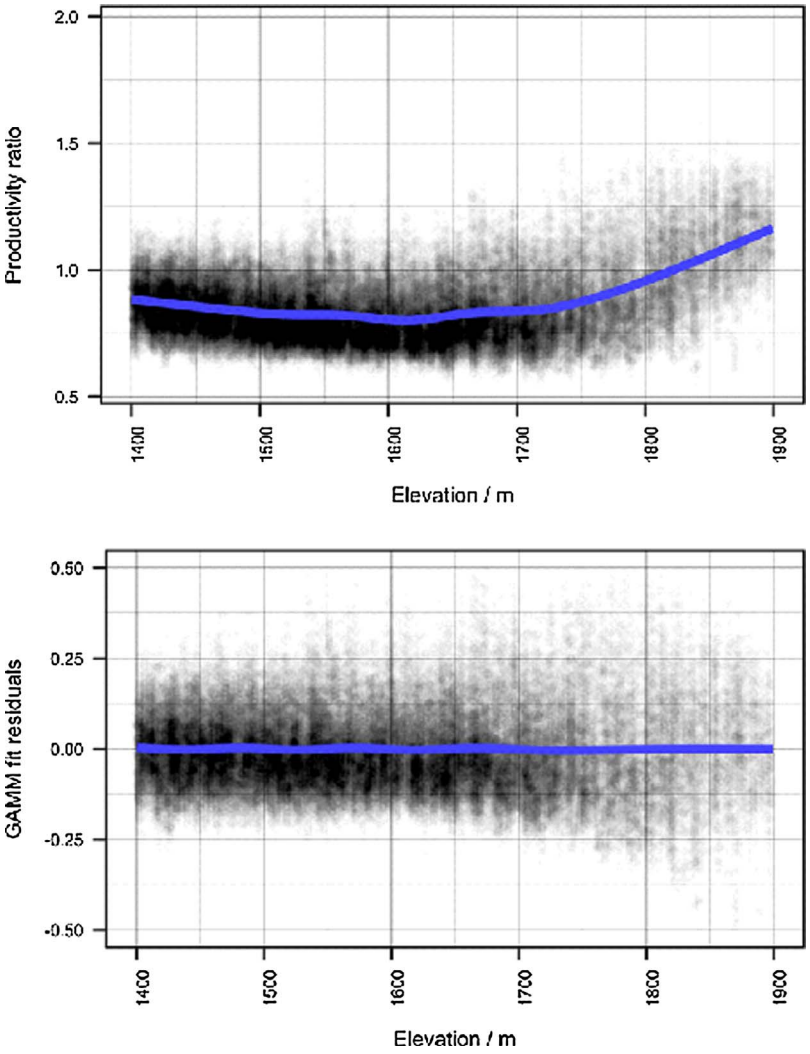

Fig. 10. Elevation effect of productivity ratio: actual data (top panel) and GAMM fit residuals (bottom panel). Both data were smoothed by loess (blue-coloured).

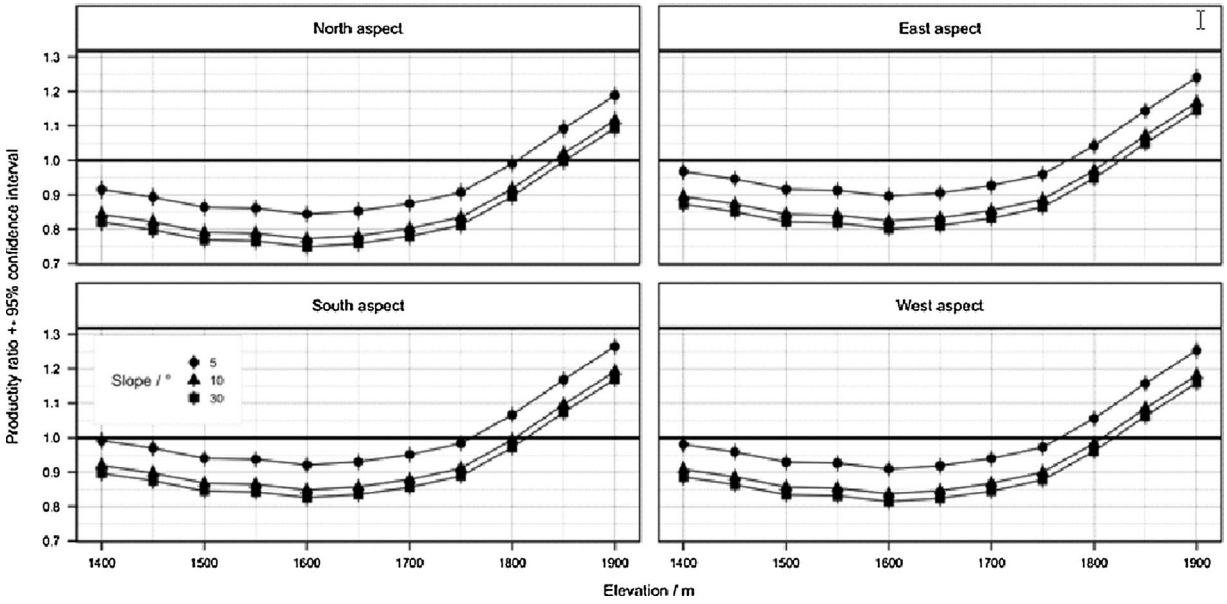

Fig. 11. GAMM fit of Productivity ratio over elevation for SFD pixels.

mid-elevations (1500–1700 m), on steep terrains and North aspects. Conversely, at higher elevations (i.e. 1850–1900 m for North-facing terrains, and 1800–1900 m for South-facing terrains), year 2016 productivity was higher than previous years despite being hit by the spring frost. This may be accounted by the more favorable climate conditions of 2016 during the growing season that enabled trees to recover the spring frost damage to foliage. Furthermore, the SFD pixels at higher elevations probably have been hit by the late frost when their greening process was at the beginning (like for NSFD pixels), so at these elevations the SFD beech stands suffered the frost impact less than at lower elevations. More factors that vary on a yearly basis may have played a role in the decrease of productivity in the 1500–1700 m range including an unprecedented absence of snow cover during the winter of 2015–2016 that, in turns, might have prompted an earlier leaf unfolding phase increasing the susceptibility of beech trees to spring frost events.

Overall, beech forests affected by the spring frost (in the range 1.400-1.900 m) reduced their productivity by 14%, relative to the 15 previous years, due to the damage caused to foliage and to a two months-long greening trend recovery period; whereas unaffected beech forests closed year 2016 with an average increase of productivity of 5%. In beech forests at lower elevations, the spring frost has turned a favorable year for growth into the least productive year since 2001.

Although the occurrence of freezing temperatures in spring is very stochastic, the period of leaf unfolding in temperate forests is under a great risk of damage due to spring frosts (Vitasse et al., 2014). Spring phenology of European common beech is well adapted to escape freeze damages on longer time scales (Lenz et al., 2013). However, winters are expected to become progressively milder, with an increasing risk of exceptionally warm spells. While there is no common agreement if the risk of freeze damages in trees will increase in the next decades under continued climate change, we noted that a unique spring frost event can significantly and largely affect the productivity of a damaged forest on a large scale.

In conclusions, satellite remote sensing, by providing a wide spatial coverage and internal consistency of data sets, allowed to detect spring frost events associated with temporal changes in productivity between damage and non-damage conditions, within and among the years. The analyses of remotely-sensed EVI data effectively provided valuable information for monitoring the status of vegetation which is an indicator of the degree of stress related to any anomalies that adversely influences plants in response to natural hazards and/or anthropogenic activities.

The ability to identify spring frost spatial dynamics is essential for understanding current and future natural and human-assisted beech forests range shifts. The proposed approach represents a step forward the use of remotely-sensed time series of greenness indices as input to automatically detect areas subject to seasonal anomalies, map their spatial patterns, and quantify the anomaly effects in terms of productivity, from local to global scale.

References

Alberton, B., Almeida, J., Helm, R., da Torres, S., Menzel, R., Morellato, A.L.P.C., 2014. Using phenological cameras to track the green up in a cerrado savanna and its on-the-ground validation. Ecol. Inf. 19, 62–70. http://dx.doi.org/10.1016/j.ecoinf.2013.12.011.

Assal, T.J., Anderson, P.J., Sibold, J., 2016. Spatial and temporal trends of drought effects in a heterogeneous semi-arid forest ecosystem. For. Ecol. Manage. 365, 137–151. http://dx.doi.org/10.1016/j.foreco.2016.01.017.

Aubinet, M., Grelle, A., Ibrom, A., Rannik, U., Moncrieff, J., Foken, T., Kowalski, A.S., Martin, P.H., Berbigier, P., Bernhofer Ch, Clement, R., Elbers, J., Granier, A., Grunwald, T., Morgenstern, K., Pilegaard, K., Rebmann, C., Snijders, W., Valentini, R., Vesala, T., 2000. Estimates of the annual net carbon and water exchange of forests: the EUROFLUX methodology. Adv. Ecol. Res. 30, 113–175.

Aubinet, M., Vesala, T., Papale, D., 2012. Eddy Covariance: a Practical Guide to Measurement and Data Analysis. Springer, London.

Augspurger, C.K., 2013. Reconstructing patterns of temperature, phenology, and frost damage over 124 years: spring damage risk is increasing. Ecology 94, 41–50. http://dx.doi.org/10.1890/12-0200.1.

Awaya, Y., Tanaka, K., Kodani, E., Nishizono, T., 2009. Responses of a beech (Fagus crenata Blume) stand to late spring frost damage in Morioka. Jpn. For. Ecol. Manage. 257, 2359–2369. http://dx.doi.org/10.1016/j.foreco.2009.03.028.

Badeck, F.-W., Bondeau, A., Böttcher, K., Doktor, D., Lucht, W., Schaber, J., Sitch, S., 2004. Responses of spring phenology to climate change. New Phytol. 162, 295–309. http://dx.doi.org/10.1111/j.1469-8137.2004.01059. x.

Bajocco, S., De Angelis, A., Salvati, L., 2012. A satellite-based green index as a proxy for vegetation cover quality in a Mediterranean region. Ecol. Indic. 23, 578–587. http://dx.doi.org/10.1016/j.ecolind.2012.05.013.

Bascietto, M., De Cinti, B., Matteucci, G., Cescatti, A., 2012. Biometric assessment of aboveground carbon pools and fluxes in three european forests by randomized branch sampling. For. Ecol. Manage. 267, 172–181.

Bolte, A., Czajkowski, T., Kompa, T., 2007. The north-eastern distribution range of European beech—a review. For.: Int. J. For. Res. 80, 413–429. http://dx.doi.org/10.1093/forestry/cpm028.

Campbell, C., Ying, Y., 2010. Learning with Support Vector Machines, Learning with Support Vector Machines. Morgan & Claypool.

Cuomo, V., Lanfredi, M., Lasaponara, R., Macchiato, M.F., Simoniello, T., 2001. Detection of interannual variation of vegetation in middle and southern Italy during 1985–1999 with 1 km NOAA AVHRR NDVI data. J. Geophys. Res. 106, 17863–17876. http://dx.doi.org/10.1029/2001JD900166.

Dallimer, M., Tang, Z., Gaston, K.J., Davies, Z.G., 2016. The extent of shifts in vegetation phenology between rural and urban areas within a human-dominated region. Ecol.

Evol. 6, 1942–1953. http://dx.doi.org/10.1002/ece3.1990.
Dittmar, C., Fricke, W., Elling, W., 2006. Impact of late frost events on radial growth of common beech (Fagus sylvatica L.) in Southern Germany. Euro. J. For. Res. 125, 249–259. http://dx.doi.org/10.1007/s10342-005-0098-y.
Fraser, R.H., Latifovic, R., 2005. Mapping insect-induced tree defoliation and mortality using coarse spatial resolution satellite imagery. Int. J. Remote Sens. 26, 193–200. http://dx.doi.org/10.1080/01431160410001716923.
Huete, A., Didan, K., Miura, T., Rodriguez, E., Gao, X., Ferreira, L., 2002. Overview of the radiometric and biophysical performance of the MODIS vegetation indices. Remote Sens. Environ. 83, 195–213. http://dx.doi.org/10.1016/S0034-4257(02)00096-2.
Hufkens, K., Friedl, M.A., Keenan, T.F., Sonnentag, O., Bailey, A., O'Keefe, J., Richardson, A.D., 2012. Ecological impacts of a widespread frost event following early spring leaf-out. Global Change Biol. 18, 2365–2377. http://dx.doi.org/10.1111/j.1365-2486.2012.02712. x.
Inouye, D.W., 2000. The ecological and evolutionary significance of frost in the context of climate change. Ecol. Lett. 3, 457–463. http://dx.doi.org/10.1046/j.1461-0248.2000.00165. x.
James, G.M., 2003. Variance and bias for general loss functions. Mach. Learn. 51, 115–135. http://dx.doi.org/10.1023/A:1022899518027.
Kim, Y., Kimball, J.S., Didan, K., Henebry, G.M., 2014. Response of vegetation growth and productivity to spring climate indicators in the conterminous United States derived from satellite remote sensing data fusion. Agric. Forest Meteorol. 194, 132–143. http://dx.doi.org/10.1016/j.agrformet.2014.04.001.
Kreyling, J., Thiel, D., Nagy, L., Jentsch, A., Huber, G., Konnert, M., Beierkuhnlein, C., 2012a. Late frost sensitivity of juvenile Fagus sylvatica L. differs between southern Germany and Bulgaria and depends on preceding air temperature. Euro. J. For. Res. 131, 717–725. http://dx.doi.org/10.1007/s10342-011-0544-y.
Kreyling, J., Stahlmann, R., Beierkuhnlein, C., 2012b. Spatial variation in leaf damage of forest trees and the regeneration after the extreme spring frost event in May 2011. Allgemeine For. Jagdzeitung 183, 15–22.
Lanfredi, M., Lasaponara, R., Simoniello, T., Cuomo, V., Macchiato, M., 2003. Multiresolution spatial characterization of land degradation phenomena in southern Italy from 1985 to 1999 using NOAA-AVHRR NDVI data. Geophys. Res. Lett. 30http://dx.doi.org/10.1029/2002gl015514. (n/a-n/a).
Lasaponara, R., 2006. On the use of principal component analysis (PCA) for evaluating interannual vegetation anomalies from SPOT/VEGETATION NDVI temporal series. Ecol. Modell. 194, 429–434. http://dx.doi.org/10.1016/j.ecolmodel.2005.10.035.
Lenz, A., Hoch, G., Vitasse, Y., Korner, C., 2013. European deciduous trees exhibit similar safety margins against damage by spring freeze events along elevational gradients. New Phytol. 200, 1166–1175. http://dx.doi.org/10.1111/nph.12452.
Leuschner, C., Meier, I.C., Hertel, D., 2006. On the niche breadth of Fagus sylvatica: soil nutrient status in 50 Central European beech stands on a broad range of bedrock types. Ann. For. Sci. 63, 355–368. http://dx.doi.org/10.1051/forest:2006016.
Lintvedt, K., 2011. Analyzing Spring Freeze Impacts on Deciduous Forest Productivity Using MODIS Satellite Imagery, Theses and Dissertations. pp. 159. http://scholarworks.uark.edu/etd/159.
MacQueen, J., 1967. Some methods for classification and analysis of multivariate observations. In: Proceedings of the Fifth Berkeley Symposium on Mathematical Statistics and Probability Volume 1: Statistics. University of California Press Berkeley, Calif. pp. 281–297.
Maeda, E.E., Heiskanen, J., Aragão, L.E.O.C., Rinne, J., 2014. Can MODIS EVI monitor ecosystem productivity in the Amazon rainforest? Geophys. Res. Lett. 41, 7176–7183. http://dx.doi.org/10.1002/2014GL061535.
Matteucci, G., Masci, A., Valentini, R., Scarascia, G., 2007. The response of forests to global change: measurements and modelling simulations in a mountain forest of the Mediterranean Region. In: In: Palahi, M., Byrot, Y., Rois, M. (Eds.), Scientific Tools and Research Needs for Multifunctional Mediterranean Forest Ecosystem Management EFI Proceedings 56. pp. 11–23.
Mazzenga, F., 2017. Analisi di lungo termine sui fattori di controllo dello scambio di carbonio in una faggeta dell'Italia centromeridionale. (PhD Thesis). Department for Innovation in Biological, Agro-food and Forest Systems. University of Tuscia, Viterbo, Italy.
Menzel, A., Fabian, P., 1999. Growing season extended in Europe. Nature 397http://dx.doi.org/10.1038/17709. (659-659).
Menzel, A., Helm, R., Zang, C., 2015. Patterns of late spring frost leaf damage and recovery in a European beech (Fagus sylvatica L.) stand in south-eastern Germany based on repeated digital photographs. Front. Plant Sci. 6, 110. http://dx.doi.org/10.3389/fpls.2015.00110.
Mildrexler, D.J., Zhao, M., Heinsch, F.A., Running, S.W., 2007. A new satellite-based methodology for continental-scale disturbance detection. Ecol. Appl. 17, 235–250. http://dx.doi.org/10.1890/1051-0761(2007)017[0235:ANSMFC]2.0.CO;2.
Muffler, L., Beierkuhnlein, C., Aas, G., Jentsch, A., Schweiger, A.H., Zohner, C., Kreyling, J., 2016. Distribution ranges and spring phenology explain late frost sensitivity in 170 woody plants from the Northern Hemisphere. Global Ecol. Biogeogr. 25, 1061–1071. http://dx.doi.org/10.1111/geb.12466.
Myneni, R.B., Williams, D.L., 1994. On the relationship between FAPAR and NDVI. Remote Sens. Environ. 49, 200–211. http://dx.doi.org/10.1016/0034-4257(94)90016-7.
Ningre, F., Colin, F., 2007. Frost damage on the terminal shoot as a risk factor of fork incidence on common beech (Fagus sylvatica L.). Ann. For. Sci. 64, 79–86. http://dx.doi.org/10.1051/forest:2006091.
Olsson, P.O., Kantola, T., Lyytikäinen-Saarenmaa, P., Jönsson, A.M., Eklundh, L., 2016. Development of a method for monitoring of insect induced forest defoliation − limitation of MODIS data in Fennoscandian forest landscapes. Silva Fennica 50. http://dx.doi.org/10.14214/sf.1495.
Potter, C., Kooster, S., Huete, A., 2007. Terrestrial carbon sinks for the United States predicted from MODIS satellite data and ecosystem modeling. Earth Interact. 11, 1–21. http://dx.doi.org/10.1175/EI228.1.
Richardson, A.D., Braswell, B.H., Hollinger, D.Y., Jenkins, J.P., Ollinger, S.V., 2009. Near-surface remote sensing of spatial and temporal variation in canopy phenology. Ecol. Appl. 19, 1417–1428. http://dx.doi.org/10.1890/08-2022.1.
Rigby, J.R., Porporato, A., 2008. Spring frost risk in a changing climate. Geophys. Res. Lett. 35http://dx.doi.org/10.1029/2008gl033955. n/a–n/a.
Rojas, O., Vrieling, A., Rembold, F., 2011. Assessing drought probability for agricultural areas in Africa with coarse resolution remote sensing imagery. Remote Sens. Environ. 115, 343–352. http://dx.doi.org/10.1016/j.rse.2010.09.006.
Rosenzweig, C., Karoly, D., Vicarelli, M., Neofotis, P., Wu, Q., Casassa, G., Menzel, A., Root, T.L., Estrella, N., Seguin, B., Tryjanowski, P., Liu, C., Rawlins, S., Imeson, A., 2008. Attributing physical and biological impacts to anthropogenic climate change. Nature 453, 353–357. http://dx.doi.org/10.1038/nature06937.
Scheifinger, H., Menzel, A., Koch, E., Peter, C., 2003. Trends of spring time frost events and phenological dates in Central Europe. Theor. Appl. Climatol. 74, 41–51. http://dx.doi.org/10.1007/s00704-002-0704-6.
Suepa, T., Qi, J., Lawawirojwong, S., Messina, J.P., 2016. Understanding spatio-temporal variation of vegetation phenology and rainfall seasonality in the monsoon Southeast Asia. Environ. Res. 147, 621–629. http://dx.doi.org/10.1016/j.envres.2016.02.005.
Van Hoek, M., Jia, L., Zhou, J., Zheng, C., Menenti, M., 2016. Early drought detection by spectral analysis of satellite time series of precipitation and normalized difference vegetation index (NDVI). Remote Sens. 8. http://dx.doi.org/10.3390/rs8050422.
Vitasse, Y., Lenz, A., Körner, C., 2014. The interaction between freezing tolerance and phenology in temperate deciduous trees. Front. Plant Sci. 5, 541. http://dx.doi.org/10.3389/fpls.2014.00541.
Wang, Z., Liu, C., Huete, A., 2003. From AVHRR-NDVI to MODIS-EVI: Advances in vegetation index research. Acta Ecol. Sin. 23, 979–987.
Yool, S.R., 2001. Enhancing fire scar anomalies in AVHRR NDVI time-Series data. Geocarto Int. 16, 7–14. http://dx.doi.org/10.1080/10106040108542177.
Zhang, Q., Xiao, X., Braswell, B., Linder, E., Ollinger, S., Smith, M.-L., Jenkins, J.P., Baret, F., Richardson, A.D., Moore III, B., Minocha, R., 2006. Characterization of seasonal variation of forest canopy in a temperate deciduous broadleaf forest, using daily MODIS data. Remote Sens. Environ. 105, 189–203. http://dx.doi.org/10.1016/j.rse.2006.06.013.
Zhou, Z.G., Tang, P., Zhou, M., 2016. Detecting anomaly regions in satellite image time series based on seasonal autocorrelation analysis: ISPRS Ann. Photogramm. Remote Sens. Spat. Inf. Sci. 303–310 (III-3).